

## Full Length Article

# A tag-and-count approach for quantifying surface silanol densities on fused silica based on atomic layer deposition and high-sensitivity low-energy ion scattering

Tahereh G. Avval<sup>a</sup>, Stanislav Průša<sup>b,c</sup>, Cody V. Cushman<sup>d</sup>, Grant T. Hodges<sup>a</sup>, Sarah Fearn<sup>e</sup>, Seong Kim<sup>f</sup>, Jan Čechal<sup>c</sup>, Elena Vaníčková<sup>c</sup>, Pavel Bábík<sup>c</sup>, Tomáš Šíkola<sup>b,c</sup>, Hidde H. Brongersma<sup>g</sup>, Matthew R. Linford<sup>a</sup>

<sup>a</sup> Department of Chemistry and Biochemistry, Brigham Young University, C100 BNSN, Provo, UT 84602, USA

<sup>b</sup> Institute of Physical Engineering, Brno University of Technology, Technická 2, Brno 616 69, Czech Republic

<sup>c</sup> CEITEC BUT, Brno University of Technology, Purkyňova 123, 612 00 Brno, Czech Republic

<sup>d</sup> Science & Technology Division, Corning Incorporated, Corning, NY 14831, USA

<sup>e</sup> Department of Materials, Imperial College of London, London SW7 2AZ, U.K

<sup>f</sup> Department of Chemical Engineering, The Pennsylvania State University, State College, PA USA

<sup>g</sup> Department of Applied Physics, Eindhoven University of Technology, 5600 MB Eindhoven, The Netherlands

## ABSTRACT

Surface silanols (SiOH) are important moieties on glass surfaces. Here we present a tag-and-count approach for determining surface silanol densities, which consists of tagging surface silanols with Zn via atomic layer deposition (ALD) followed by detection of the zinc by high sensitivity-low energy ion scattering (HS-LEIS). Shards of fused silica were hydroxylated with aqueous hydrofluoric acid (HF) and then heated to 200, 500, 700, or 900 °C. These heat treatments increasingly condense and remove surface silanols. The samples then underwent one ALD cycle with dimethylzinc (DMZ) or diethylzinc (DEZ) followed by water. As expected, fused silica surfaces heated to higher temperatures showed lower Zn coverages. When fused silica surfaces treated at 200 °C were exposed to DMZ for two different times, the same sub-monolayer quantity of Zn was obtained by X-ray photoelectron spectroscopy (XPS). Surface cleaning/preparation immediately before HS-LEIS, including atomic oxygen treatment and annealing, played a critical role in these efforts. Surfaces treated with DMZ generally showed slightly higher Zn signals by LEIS. Using this methodology, a value of 4.59 OH/nm<sup>2</sup> was found for fully hydroxylated fused silica. Both this result and those obtained at 500, 700, and 900 °C are in very good agreement with literature values.

## 1. Introduction

The flat panel displays (FPDs) found in cell phones, televisions, and computers are a crucial part of modern technology, [1] where the need for FPDs in multiple applications will likely increase in the future [2]. Thus, market demand will continue to drive innovation in FPD manufacturing, such that they will become thinner, stronger, cheaper, and have higher resolution. Glass is the most important substrate for FPD manufacturing, where both its bulk and surface properties are critical for its performance. Indeed, many properties of the glass used in FPDs are controlled by its surface chemistry. For example, static discharge, which is affected by factors that include surface cleanliness and particle adhesion, can result in FPD failure and lower device yield [3–6]. These issues are becoming more important as pixel dimensions decrease [2,7]. Glass surface chemistry is also altered by various treatments on the production line; glass substrates undergo multiple chemical treatments before they are suitable for FPD production [8,9].

Surface hydroxyls are the most important functional groups on a glass surface. Indeed, these moieties play a critical role in most adsorption and surface-mediated processes that occur on oxide surfaces, including wetting, adhesion, and the rate of contamination. They also affect electrostatic charging and discharging on these surfaces. Accordingly, understanding the surface hydroxyl density and how it changes during industrial processing is fundamental to (i) understanding display glass surface properties, and (ii) improving surface-mediated performance attributes [4,10,11,12]. Because of the significant role silanols play in surface glass chemistry, there is interest in their quantification and modification to produce oxide materials with increased functionality and value for a wide variety of products [13].

Fundamental studies on surface silanols in the literature have been performed with various analytical techniques, including infrared spectroscopy (FTIR), gravimetric analysis, Brunauer-Emmett-Teller (BET) surface area measurements, and temperature-programmed desorption mass spectrometry (TPD-MS). Much of this early work was done on

E-mail address: [mrlinford@chem.byu.edu](mailto:mrlinford@chem.byu.edu) (M.R. Linford).

<https://doi.org/10.1016/j.apsusc.2022.154551>

Received 14 June 2022; Received in revised form 1 August 2022; Accepted 11 August 2022  
0169-4332/© 20XX

high-surface area silica in powder, fiber, and gel forms [3,10,12,14,15]. For instance, FTIR revealed that there are different types of surface silanols, including geminal, isolated, and bridged silanols, where each has a different reactivity due to different degrees of hydrogen bonding [12]. Other studies have focused on quantifying the density of these functional groups at surfaces [14]. A number of these attempts were summarized in a review article that proposed the Zhuravlev model that describes the degree of hydroxylation on silica surfaces based on a comprehensive study of more than a hundred silica powder samples [12, 16]. According to this model, a fully-hydroxylated, amorphous silica surface has 4.6 OH groups/nm<sup>2</sup>. However, this degree of hydroxylation changes based on the thermal history of the sample. Commenting on the silica surface, Hall observed: “Up to approximately 165 °C, only physically adsorbed water is removed from the surface of the silica. Between 165 °C and about 400 °C hydroxyl groups are thermally removed from the surface and these can be replaced by re-exposure to water. Above 400 °C, hydroxyl groups continue to be removed from the surface as the temperature of dehydration is increased. However, as the pretreatment temperature increases, a decreasing number of groups can be reformed on the surface until, at about 800 °C, re-addition of water is futile and the dehydration process is irreversible.” [17] Nevertheless, even after heating to 900 °C, silanols are still present on silica – only after treatment at 1200 °C are the silanols completely gone [18,19]. According to Zhuravlev, the threshold temperature for removing all of the physisorbed water on silica without removing/disturbing surface silanols is 190 ± 10 °C [12]. Other authors including Zhuravlev have noted that (i) at room temperature, silica surfaces are typically covered with adsorbed water from the atmosphere, and (ii) heating *in vacuo* at ca. 200 °C completely removes these water molecules from the surface [10,12,20]. On a planar surface *in vacuo*, it requires ca. 2.5 hrs at this temperature to remove the physisorbed water [21].

While previous studies on high surface area samples (powder) greatly expanded our understanding of surface hydroxyls, these materials may not fully represent planar surfaces [10,22]. In addition, some of the traditional techniques used in the aforementioned studies are bulk sensitive and therefore not applicable to low surface area planar surfaces. Recently, various researchers, including some of the authors on this paper, have quantified the density of silanols on planar surfaces using surface sensitive analytical techniques such as time-of-flight secondary ion mass spectrometry (ToF-SIMS) [10,23], X-ray photoelectron spectroscopy (XPS), attenuated total internal reflectance infrared spectroscopy (ATR-IR) [24], and sum frequency generation spectroscopy [25]. Among these methods, SIMS was advantageous because it can detect hydrogen. Nevertheless, SIMS is limited in its ability to produce quantitative information. While XPS is more quantitative, it is also less surface sensitive. Attempts have been made to peak fit the XPS O 1s envelope to resolve signal contributions from surface hydroxyls, non-bridging oxygen atoms, and bridging oxygen atoms [26]. However, such approaches may not be fully reliable due to the relatively small chemical shifts in the O 1s spectrum for these different types of oxygen species and/or the large amount of bulk oxygen signal in these peak envelopes [27]. Indeed, the SIMS and XPS signals appear to be averages over a few atomic layers. In contrast, low energy ion scattering (LEIS) is the only surface analytical tool with the ability to selectively detect and quantify the outermost atomic layer of a material [28,29]. For this reason, LEIS is becoming increasingly important in catalysis studies [30] and other areas of surface science, including atomic layer deposition (ALD). High sensitivity LEIS (HS-LEIS) refers to LEIS performed on modern instrumentation, which has significantly increased the signal-to-noise ratios in measurements [28,31].

Chemical derivatization followed by surface characterization (tag-and-count) is an approach for indirectly quantifying surface silanols. Here, surface moieties are tagged via chemical reactions to better differentiate surface signals from bulk signals. Surface sensitive techniques like XPS are then used to quantify the amount of label/het-

eroatom [4,6,27,32]. Tagging agents in these studies have included silanes with cyano and CF<sub>3</sub> groups. Silane tagging agents react selectively with hydroxyl groups, where, for example, fluorinated silanes generally introduce/tag surfaces with multiple fluorine atoms, which have a high cross-section in XPS [27]. Challenges of this approach include the steric limitations of the tags, incomplete reactions, and the effects/reactivity of physisorbed water [33].

In this work, we propose a tag-and-count approach that consists of coupling atomic layer deposition (ALD) with LEIS to quantify the density of surface silanols on fused silica glasses (see Fig. 1). First, using chemical and thermal treatments, samples with different densities of surface silanols were created. The silanols on these surfaces were then reacted with an organometallic reagent (an ALD precursor), which tags the silanols with a metal atom. ALD is a process by which surface layers of generally submonolayer to monolayer dimensions are added to a substrate in a highly controlled manner via the alternating deposition of precursors [34]. For example, a reliable and much-studied ALD reaction/system is the deposition of Al<sub>2</sub>O<sub>3</sub> from trimethylaluminum (TMA) and water [34,35]. In a similar fashion, zinc oxide (ZnO) thin films can be prepared by ALD from water and either zinc acetate, dimethylzinc (DMZ), or diethylzinc (DEZ) [36]. Both DMZ and DEZ are extremely reactive precursors [37]. (We see it as slightly ironic that DEZ is used as a source of ethyl groups in organic chemistry, but for zinc in ALD.) In an ALD process, the early stages of film formation, termed the transient regime, may be nonlinear, involving three-dimensional growth that depends on substrate reactivity, i.e., the growth in this regime is highly dependent on the functional groups at the surface [38]. In this work here, dehydrated, fused silica surfaces with different densities of silanol groups were tagged with Al and Zn. Two zinc precursors with different sizes (DMZ and DEZ) were used to investigate steric effects. The Al-tagged surfaces were characterized by XPS and spectroscopic ellipsometry (SE), and the Zn-tagged surfaces were characterized with XPS and LEIS. Different sample cleaning procedures were investigated in the LEIS analyses. Fused silica surfaces that had been treated with DMZ for different lengths of time were also studied. That the same amount of Zn was obtained at different exposure times suggests that DMZ is neither reacting with surface siloxanes nor decomposing on the surface. We believe that our approach will be useful as a general methodology for tagging and counting surface silanols on inorganic surfaces. In addition, it

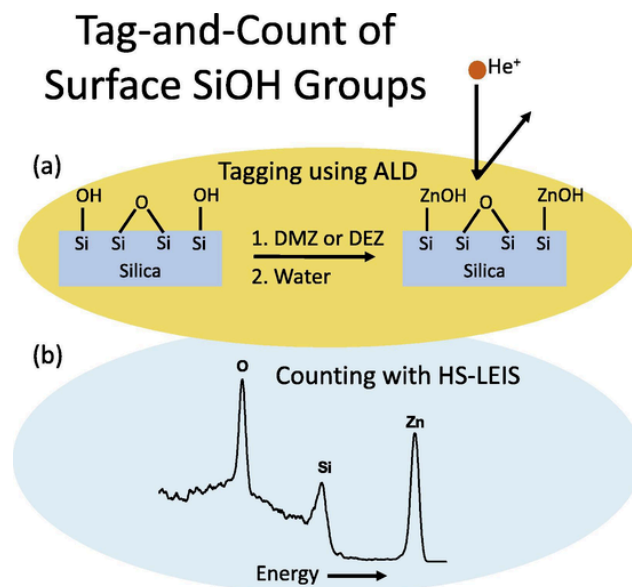


Fig. 1. Schematic of the tag-and-count approach proposed in this work. (a) Tagging of surface silanols with ALD reagents via one cycle of dimethylzinc (DMZ) or diethylzinc (DEZ) and water, and (b) Counting the tagged silanols (zinc atoms) using HS-LEIS.

could be used to study the initial stages of ALD growth more extensively, and for ALD in general. To the best of our knowledge, this is the first report of tagging a silanol-containing surface with ALD and counting the resulting atoms with LEIS.

## 2. Experimental

### 2.1. Reagents

Fused silica slides (GE 124, Type-I silica) were purchased from Structure Probe Incorporated (SPI Supplies, Westchester, PA). HF, ACS grade, was purchased from EMD. The ALD precursors, (TMA, DMZ and DEZ) were obtained from Strem Chemicals (Newburyport, MA, USA). The water used in the ALD process was HPLC grade.

### 2.2. Sample preparation

Samples for this study included chemically and thermally treated fused silica slides. The chemical treatment of the fused silica surfaces was to immerse them in 0.1 M HF in a 50 mL perfluorocarbon container at room temperature for 10 min. Immediately after chemical treatment, the solution contents of the container were exchanged five times with deionized water to quench the reaction, after which the sample was extracted with tweezers, rinsed under a spray of deionized water for ca. 1 min, and finally blown dry with nitrogen. Prior to chemical treatment, the back sides of the slides were roughened with a sand blaster, which was done to mark one side of the samples and also to suppress backside reflections in subsequent spectroscopic ellipsometry (SE) measurements [39]. Immediately after chemical or thermal treatment, all samples were placed in clean, airtight glass vials with UHV-foil-lined caps to preserve them until they could be analyzed. For example, HF-treated pieces of fused silica were stored in this way 1–2 h prior to heat treatments, which were performed in the air at 200, 500, 700 and 900 °C. ALD tagging was performed on multiple pieces of silica treated at these four different temperatures, which were first dehydrated in the ALD system at 200 °C for 2.5 h. They then underwent one complete ALD cycle to tag the surface silanols, which consisted of a single dose of TMA, DMZ, or DEZ, followed by a dose of water (see Table 1).

### 2.3. Reference preparation

Quantification in LEIS is straightforward with appropriate reference materials. The reference samples for this study were as-received fused silica for silicon and a thick film of ZnO on fused silica deposited by ALD for zinc. To prepare the zinc reference, a fused silica slide was (i) treated with HF (0.1 M for 10 min), (ii) dehydrated in the ALD chamber for 2.5 h at 200 °C, and (iii) a ca. 20 nm ZnO film was then deposited on it from 150 ALD cycles of DMZ and water. The DMZ dose time, N<sub>2</sub>(g) purge time, water dose time, and N<sub>2</sub>(g) purge time for one ALD cycle in this deposition were 21.0 ms, 10.0 s, 15.5 ms, 10.0 s, respectively. The same procedure was employed to prepare a thick ZnO film from DEZ.

**Table 1**  
Experimental process parameters for the ALD depositions.

Sample Type	Reagent	Dose Time (ms)	Purge Time (s)
All	TMA	21.0	15.0
	H <sub>2</sub> O	15.5	15.0
Tagged/Single cycle	DEZ	50.0	50.0
	H <sub>2</sub> O	50.0	50.0
Reference/Multiple cycles	DEZ	21.0	10.0
	H <sub>2</sub> O	15.5	10.0
Tagged/Single cycle	DMZ	50.0	50.0
	H <sub>2</sub> O	50.0	50.0
Reference/Multiple cycles	DMZ	21.0	10.0
	H <sub>2</sub> O	15.5	10.0

However, this film produced a lower Zn signal in LEIS compared to the film made by DMZ, presumably because of greater steric hindrance in the ethyl ligands – the quality of the ZnO surface prepared by DEZ does not appear to be as high as that made with DMZ, although the bulk properties of the films, as measured by ellipsometry, seem to be the same (vide infra). The experimental processes for both tagging samples and preparing thicker ALD films is summarized in Table 1.

### 2.4. Instrumentation

#### 2.4.1. Atomic layer deposition (ALD)

ALD was performed with a Kurt J. Lesker (Jefferson Hills, PA) ALD-150LX™ system. For the Al depositions, the TMA reagent was at room temperature, and the depositions were performed at 200 °C. For the Zn depositions, the temperature of the precursors was 110 °C, and the depositions were also performed at 200 °C.

#### 2.4.2. X-ray photoelectron spectroscopy (XPS)

XPS of the alumina-on-silica samples was performed with a Surface Science SSX-100 X-ray photoelectron spectrometer (serviced by Service Physics, Bend, OR) with a monochromatic Al K $\alpha$  source, a hemispherical analyzer, and a take-off angle of 35°. Survey scans were recorded with a spot size of 800 × 800  $\mu\text{m}^2$  and a resolution of 4 (nominal pass energy of 150 eV). In addition to a fine nickel mesh directly above the sample, an electron flood gun was employed for charge compensation. The narrow scans collected were the average of 20 individual scans. The same measurement was performed at three different spots on each sample. XPS peaks were referenced to the C 1s hydrocarbon signal (taken to be at 285.0 eV) [40]. While the C 1s peak is a less-than-ideal reference, it is often helpful in identifying peaks. XPS of the ZnO-on-silica samples was performed on a SPECS system equipped with a Phoibos 150 spectrometer with a microchannel plate detector with a 2D CCD camera. Non-monochromatized Mg K $\alpha$  radiation with 300 W emission power (12.5 kV cathode–anode voltage) and normal emission geometry (emission angle 0°) were employed for all measurements. A survey spectrum was measured in high magnification mode using a pass energy of 100 eV by integration of 2 sweeps with dwell times of 0.1 s and energy steps of 1 eV. Zn 2p, Zn LMM, O 1s, C 1s, and Si 2p detail spectra were acquired in high magnification mode using a pass energy of 20 eV that combined 30 (Zn LMM), 20 (Zn 2p), or 10 (all other peaks) sweeps with dwell times of 0.1 s and energy steps of 0.1 eV. The areas of the Al 2p [41] and Si 2p XPS signals were measured over linear backgrounds with CasaXPS (Casa Software Ltd., Version 2.3.18PR1.0) [42] and ratioed. Linear backgrounds are often appropriate in XPS peak fitting when there is no rise in the background. This situation often occurs with wide band gap materials [43].

#### 2.4.3. Ellipsometry

The thicknesses of alumina ALD films and native oxide layers on silicon, and also the optical constants of fused silica substrates were determined by ex situ spectroscopic ellipsometry (SE) using an M-2000DI ellipsometer with the CompleteEase® software package (J.A. Woollam, Lincoln, NE). To obtain the SE optical constants for fused silica, the SE data from hydroxylated fused silica samples that had been treated at 200, 500, 700, or 900 °C were modeled with a Sellmeier model (the starting point for this model was a Sellmeier model for fused silica glass in the instrument software, where the parameters in this model were fit). All of these samples produced essentially identical results. Prior to SE, the backside of the fused silica substrates were roughened by sandblasting to decrease/eliminate backside reflections, which would otherwise complicate the data analysis [39]. The optical constants for alumina in our instrument software were used without modification to model our alumina ALD layers. They are based on a Cody-Lorentz model.

In situ ellipsometry (during ALD growth) and analysis of this data were performed with a four-wavelength instrument and accompanying instrument software package from FilmSense (FS-1®, Lincoln, Nebraska). The in situ data from ZnO films grown from 150 cycles of DMZ or DEZ and water were fitted using a model that had layers for the silicon substrate ('Si-temp', which accounted for the variation in the optical constants of silicon with temperature), the native oxide layer (the thickness of which was obtained from ex situ ellipsometry prior to the ALD deposition), and a Cauchy layer for the ZnO films. The only parameters in this model were the thicknesses of the growing ZnO films and the two Cauchy parameters describing their index of refraction – in our model, all the growing films had the same optical constants. The tabulated optical constants for ZnO in our ex situ instrument software show that, over the wavelength range of our in situ instrument, ZnO (i) has essentially no absorption and (ii) exhibits normal dispersion, which justify the use of a Cauchy model for this material. Thus, the two Cauchy parameters and 20 thicknesses of the growing film were simultaneously fit in a multi-sample analysis (MSA), where these data points primarily came from the end of the deposition where the Cauchy model has the greatest validity.

#### 2.4.4. High Sensitivity-Low energy ion scattering (HS-LEIS)

Ion scattering experiments were performed with a high sensitivity Qtac100 (IonTof GmbH, Germany) instrument. Focused primary beams of He and Ne ions were scanned over a selected area of  $2 \times 2 \text{ mm}^2$ . The ions scattered at  $145^\circ$  were collected over the full azimuth. The incident ion beam was perpendicular to the surface plane for all presented results. The primary kinetic energy for He was 3.0 keV. The surface charging of fused silica, and the DMZ and DEZ samples, was compensated by an electron flood gun. The experimental conditions and sample surface preparation were optimized during preliminary experiments on a separate set of samples. While 4.0 keV Ne scattering gives a good Zn signal, 3.0 keV He can also monitor the signals of the other lighter elements in the system (Si, O, and C), i.e., it can detect carbon contamination. Accordingly, 3 keV He ions were used in this study. The samples were mounted on a holder that had a heating element below it. A thermocouple was pressed onto the surface to be analysed with a molybdenum spring. Each sample was measured under the following conditions: as received at RT, after atomic oxygen treatment for 30 min, and after annealing at  $270^\circ\text{C}$  for 5 min. A 20 min treatment with atomic oxygen removes most of the organic surface contamination. This treatment was performed with a microwave atom plasma cracker source (MPS-ECR, SPECS GmbH), configured for neutral atom operation, operated at a distance of 100 mm from the sample surface at 30 mA and 32 % MFC (the  $\text{O}_2$  flow rate was 0.22 sccm). The ion fluence for the 3.0 keV He spectra shown herein was  $5 \times 10^{14}$  ions/cm<sup>2</sup>, and the pressure during annealing was initially kept below  $5 \times 10^{-7}$  mbar (below  $4 \times 10^{-8}$  mbar at temperatures above  $150^\circ\text{C}$ ). All measurements were performed on the roughened (sandblasted) sides of the samples because it was easier to focus the laser, i.e., position/align the samples in the instrument. In the previous ALD depositions, the rough sides of these samples faced down. However, both XPS and LEIS confirmed that the amount of material deposited by ALD was the same whether the sample faced up or down during the deposition.

### 3. Results and discussion

#### 3.1. Tagging/ALD of chemically and thermally treated fused silica surfaces with alumina/aluminum (from TMA and water)

To understand whether ALD reagents can both tag surface silanol groups and differentiate between surfaces with different numbers of silanols, a single ALD cycle of TMA and water was applied to fully hydroxylated fused silica surfaces that had been heated to 200, 500, 700, or  $900^\circ\text{C}$  for 2.5 h. Fig. 2 shows the results of these experiments. Here,

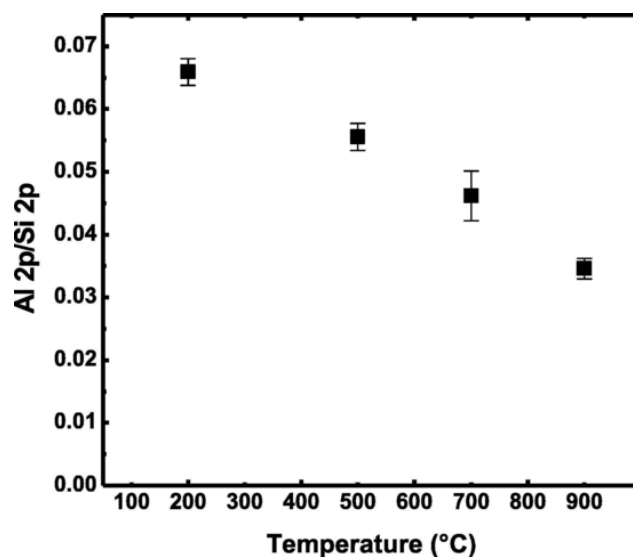


Fig. 2. XPS Al 2p/Si 2p ratios obtained after a single dose of TMA and water on HF-treated silica surfaces heated for 2.5 h at the temperature indicated in the figure. The error bars are the standard deviations of three measurements at three different spots on each sample.

the Al 2p/Si 2p XPS area ratio decreases steadily as a function of the temperature at which the fused silica surface was heated. These results suggest that single ALD cycles can differentiate between surfaces with different densities of silanol groups.

To understand the effect of initial surface silanol density on the growth of thicker ALD films, alumina films were deposited via 5, 15, 30 and 50 ALD cycles of TMA and water on fused silica surfaces that had been treated at 200, 500, 700, or  $900^\circ\text{C}$  for 2.5 h. In addition to XPS, these samples were characterized by SE to determine the thicknesses of the  $\text{Al}_2\text{O}_3$  layers. A simple two-layer SE model was employed here, which consisted of a fused silica glass layer (the substrate) and an alumina layer on top of it. The thickness of the alumina layer was the only fit parameter in the model. It would be difficult to justify a more complex model because of the known correlation between film thickness and optical constants for very thin transparent films.<sup>19, [44]</sup> The results from this analysis agree with those from XPS (see Fig. 3a). They show that the higher temperature pretreatments consistently lead to somewhat thinner films even after many ALD cycles. That is, they reveal that the initial surface chemistry has a direct impact/influence on subsequent ALD film growth. Similar effects have previously been reported. [45] The Al 2p/Si 2p ratio in Fig. 3a does not increase linearly as a function of the number of ALD cycles because XPS is most sensitive to the outermost layer of the material. In contrast, the alumina thicknesses reported in Fig. 3b do increase linearly with the ALD cycle number.

#### 3.2. Introduction to the idea of tagging surface silanols with ZnO and counting them with LEIS

While the XPS and SE results in Figs. 2 and 3 suggest that we can control the surface silanol density and subsequent ALD film growth, neither XPS nor SE is ideally suited for surface silanol quantification. SE is a model-based approach that often provides results that are more precise than accurate. For example, as a consequence of the imperfect model used here, the SE results for three of the surfaces treated with one ALD cycle of TMA and water showed slightly negative thicknesses. These results were omitted from Fig. 3b because they are obviously unphysical. As noted above, quantitative surface hydroxyl measurements with XPS are similarly challenging because (i) XPS quantitation is often based on ratios of elements, (ii) XPS does not directly detect hydrogen,

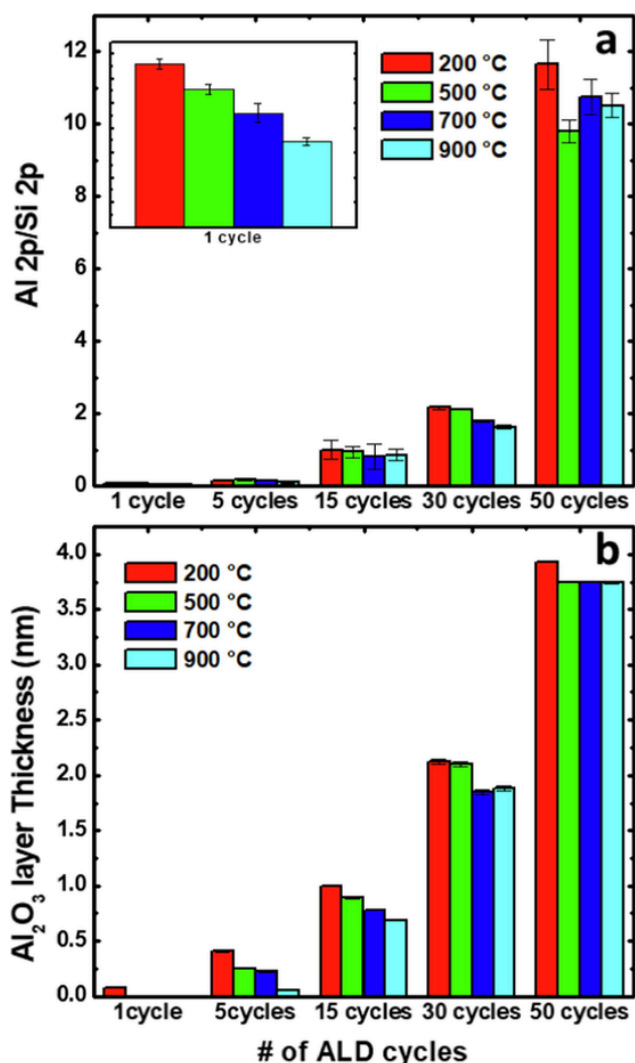


Fig. 3. (a) XPS Al 2p/Si 2p ratios and (b) SE thicknesses of ALD alumina layers on fused silica surfaces created via the number of TMA and water cycles indicated in the figure, where the fused silica surfaces had previously been heated to 200, 500, 700, or 900 °C for 2.5 h. Unphysical results (negative thicknesses) for samples prepared with 1 ALD cycle are omitted from Fig. 3b. These are a consequence of the simple SE model that was used.

(iii) oxygen only shows a limited range of chemical shifts, and (iv) XPS probes fairly deeply into materials (5 – 10 nm).

HS-LEIS is a highly surface sensitive technique that is both precise and accurate. LEIS signals primarily come from the outermost atomic layer of a material, where the technique is most often based on the scattering of incident noble gas ions from surfaces, and it is largely described by classical physics (conservation of energy and momentum). Thus, atoms with similar masses yield signals (backscattered ions) with similar energies in LEIS. In the case at hand, Si and Al (atomic masses of 28 and 27 amu, respectively) give substantially overlapping LEIS signals. While some of us recently showed that these two signals can be quantified by peak fitting [9], a better scenario for tagging and counting surface silanols would be for the tag atom to have a substantially higher mass than the other atoms in the material. This would separate its signal from the others and also give it a low background. Accordingly, we propose here a tag-and-count method based on reacting DMZ or DEZ with surface silanols to tag them with heavier zinc atoms (masses of the stable isotopes: 64 – 70 amu) that can be well detected by LEIS. Even though these reagents are relatively small, their different sizes provide an opportunity to study steric effects in these reactions

(DMZ has two methyl groups vs DEZ, which has two larger ethyl groups). We now describe the growth of thick ZnO films by ALD, discuss the necessary sample cleaning for successful HS-LEIS of Zn-tagged surfaces, report the tagging of heated fused silica surfaces with DMZ and DEZ, and finally calculate the density of surface silanols on different fused silica samples.

### 3.3. Growth of thick ZnO films by ALD

Thick ZnO films were deposited from DMZ and DEZ precursors. In particular, ca. 25 nm ZnO films were deposited on silicon shards as described above in Section 2.3 and Table 1. The rate of deposition for these two precursors (DMZ and DEZ) was determined from both in situ and ex situ ellipsometry, where ex situ SE was performed before and after ALD. The ellipsometric models for this work included the native oxide layer on silicon. For the in situ measurements, the native oxide layer was first determined by ex situ SE. The in situ model accounted for the temperature of the silicon substrate (200 °C) during the deposition, i.e., the change in the optical constants of the material with the change in temperature. For the in situ measurements, the optical constants of the ZnO film were described with a Cauchy model, which was obtained in a multi-sample analysis (MSA) of twenty measurements taken at different film thicknesses, starting at 10 nm. This approach avoided fit parameter correlation. This procedure was applied to films made with both precursors. Fig. 4 shows the resulting ZnO film thicknesses as a function of cycle number obtained from in situ ellipsometry. Here we see that under the same deposition conditions, DMZ consistently results in slightly thicker films, i.e., the rate of deposition is higher for DMZ compared to DEZ. This difference in thickness is attributed to less steric hindrance in DMZ. That is, DMZ appears to be able to react a little more with hydroxyls than DEZ. Thus, when tagging surface silanols, one would expect somewhat better results with DMZ.

The refractive indices for the ZnO films made with the two precursors are reported in Table 2. The very similar indices of refraction for these materials suggests that, at a bulk level, they are very similar.

### 3.4. Surface cleaning prior to LEIS

Hydrocarbons, including adventitious surface contamination, result in a loss of signal in LEIS because the hydrogen in the hydrocarbon leads to forward scattering of the noble gas ions. Since our LEIS analysis

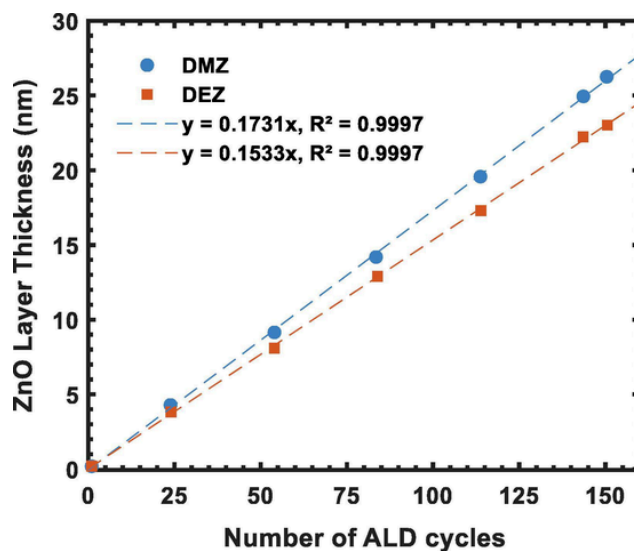


Fig. 4. Thicknesses of ZnO ALD films grown from DMZ and DEZ (and water) precursors as a function of ALD cycle number, as measured by in situ ellipsometry. Linear fits to the results with forced intercepts of zero are given in the plot.

**Table 2**

$n(\lambda)$  values at the four wavelengths used by our in situ FS-1® ellipsometer for ZnO films grown via ALD from DEZ and DMZ (and water) precursors.

$\lambda$ (nm)	$n(\lambda)$ , DEZ	$n(\lambda)$ , DMZ
466.08	2.003	2.003
524.31	1.947	1.941
598.9	1.897	1.887
636.79	1.878	1.866

is done ex situ (at a different location than the sample preparation) some contamination during sample transportation is unavoidable. Also, it is known that, depending on the precise reaction conditions, carbon and hydrogen from unreacted methyl and ethyl groups of DMZ and DEZ precursors, respectively, is incorporated into ZnO films. [46] Therefore, sample cleaning is an essential part of most LEIS measurements, including here, and various cleaning methods were tested in this study. First, the surfaces were cleaned with atomic oxygen (AO) for 10 – 30 min. Surprisingly, the LEIS signals for Zn after these treatments were not fully reproducible and often decreased after reaching a maximum. This is unusual for LEIS. It appeared that, for Zn, the AO treatment does more than just remove organic contamination. Indeed, two oxides are known for zinc: ZnO and ZnO<sub>2</sub>. ZnO is a very stable compound (m.p. 1975 °C), while ZnO<sub>2</sub> is stable at room temperature, but decomposes around 230 °C. [47] ZnO<sub>2</sub> can be synthesized through the reaction of a compound like ZnCl<sub>2</sub> with hydrogen peroxide (H<sub>2</sub>O<sub>2</sub>). [47] Since AO is even more reactive than H<sub>2</sub>O<sub>2</sub>, it is likely that AO converts ZnO to ZnO<sub>2</sub>. In LEIS, the second oxygen atom in ZnO<sub>2</sub> will also contribute to the shielding of the Zn, which explains the decreased Zn signal after long AO treatment. To obtain a well-defined oxidation state for zinc (ZnO), the samples were heated to 270 °C after exposure to AO. This treatment increases the Zn signal, which then has a stable, well-defined value. In situ XPS of the AO treated surfaces (vacuum was not broken between the AO treatment and the XPS analysis) confirmed that the AO cleaning procedure oxidized the Zn atoms in ZnO to ZnO<sub>2</sub>, as evidenced by a + 0.5 eV shift in the Zn 2p peak [46,47]. This shift is also shown in the XPS Handbook of Physical Electronics. [48].

### 3.5. Silanol tagging with ZnO

Surface silanols on fused silica surfaces were tagged with two precursors of different sizes: DMZ and DEZ (see Table 1 for experimental details). In particular, Fig. 5 shows LEIS spectra from eight different fused silica samples that were heated to 200, 500, 700, or 900 °C for 2.5 h, tagged with DMZ or DEZ, and analyzed with 3 keV He<sup>+</sup> ions by LEIS. In these results, surfaces that were treated at higher temperatures, which should have fewer silanols, show less zinc. In addition, samples that were prepared with DMZ consistently show slightly higher zinc signals than the ones prepared with DEZ (see, for example, Fig. 5c). For steric reasons, DMZ should be both the more reactive precursor and also the one that is more able to react with ‘hard to access’ silanols. The consistency and trends between the results for DMZ and DEZ in Fig. 6 suggests that they are correct.

### 3.6. Determination of surface silanol density on planar fused silica

The goal of this work is to develop a straightforward method for the quantification of surface hydroxyls on planar surfaces. In previous work, such calculations have often included the widely accepted literature value of 4.6 OH/nm<sup>2</sup> for a fully hydroxylated fused silica surface. [12] Our approach eliminates the need for such a value, enabling us to directly measure the surface silanol density. Here, the surface coverages for each element ( $\vartheta$  ZnO ( $\frac{Zn_i}{Zn_{ref}}$ ) and  $\vartheta$  SiO<sub>2</sub> ( $\frac{Si_i}{Si_{ref}}$ )) are obtained from the ratios of the signals from the samples,  $Zn_i$  and  $Si_i$ , to those from the reference materials,  $Zn_{ref}$  and  $Si_{ref}$ , which, again, are a film of ZnO grown

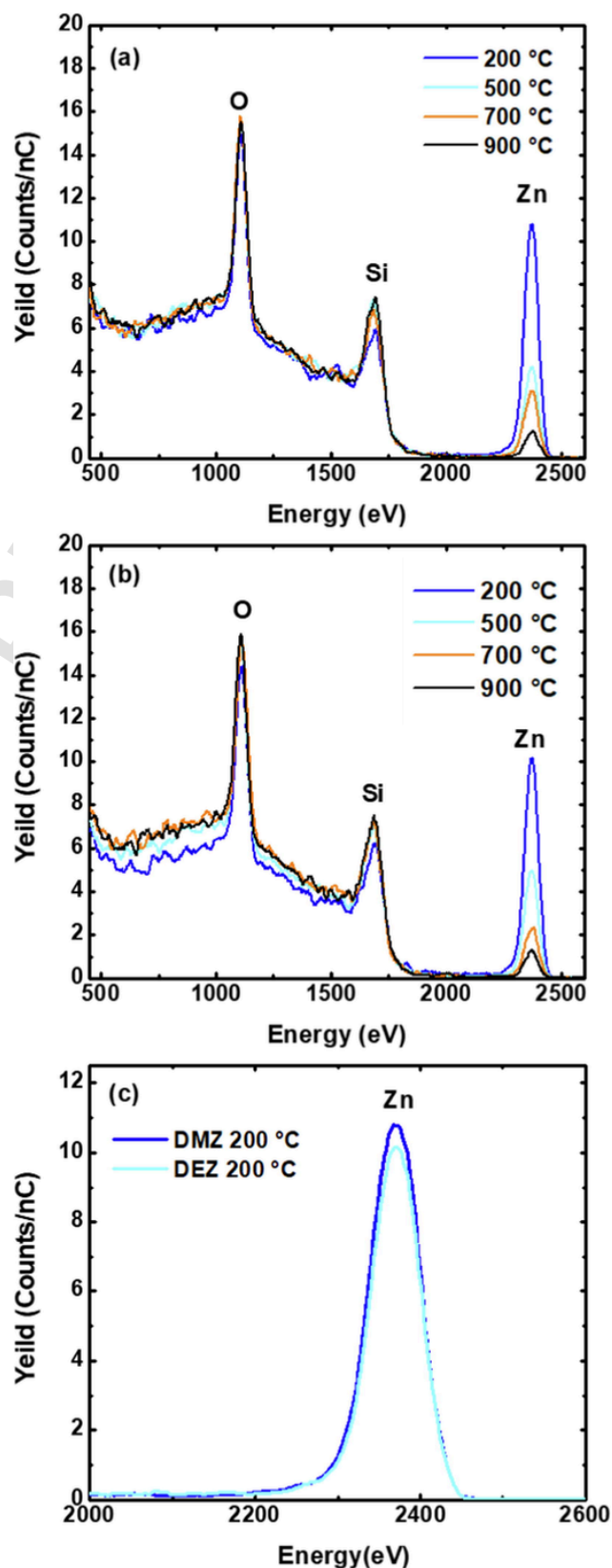


Fig. 5. LEIS spectra of fused silica surfaces treated with single doses of (a) DMZ and water and (b) DEZ and water. (c) Comparison of the zinc signals for the fused silica samples treated at 200 °C in (a) and (b) and tagged with DMZ and DEZ. All the samples were cleaned with atomic oxygen and then heated to 270 °C prior to measurement with 3 keV He<sup>+</sup>.

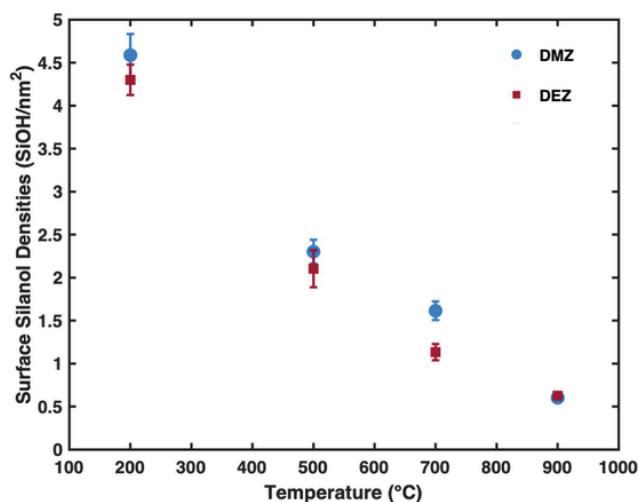


Fig. 6. Densities of surface silanols on fused silica surfaces treated at different temperatures and tagged with DMZ or DEZ, as calculated with Equation (1).

by ALD for zinc and a bare fused silica sample for silicon. The surface silanol concentration was then obtained by multiplying the normalized surface coverage for zinc oxide,  $\frac{\vartheta_{\text{ZnO}}}{\vartheta_{\text{ZnO}} + \vartheta_{\text{SiO}_2}}$ , by the ZnO areal density,  $\sigma_{\text{ZnO}}$ , as follows:

$$\text{SiOH}/\text{nm}^2 = \frac{\vartheta_{\text{ZnO}}}{\vartheta_{\text{ZnO}} + \vartheta_{\text{SiO}_2}} * \sigma_{\text{ZnO}} \left( \frac{\text{atom}}{\text{nm}^2} \right) \quad (1)$$

where  $\sigma_{\text{ZnO}}$  (11.98 ZnO unit/nm<sup>2</sup>) was derived from the literature value of the density of the material (5.606 g/cm<sup>3</sup>) [46,49]. The raw (and processed) zinc signals used in these calculations are listed in Table 2. Fig. 6 shows the results of these calculations for fused silica surfaces tagged with DMZ and DEZ. The literature value of 4.6 OH/nm<sup>2</sup> is indicated in the figure as a reference. The values obtained from DMZ and DEZ on fused silica treated at 200 °C (4.59 and 4.30 OH/nm<sup>2</sup>, respectively) are close to the literature value. In other words, especially for the smaller probe (DMZ), where its very close proximity to the accepted literature value may be a little fortuitous, there is excellent agreement between the literature value and the one obtained with our methodology. However, not only are the results at 200 °C in good agreement with literature values, the remaining results in Fig. 6 and Table 3 from the 500, 700, and 900 °C samples are also in very good agreement with the band of results presented by Zhuravlev for various silica samples. [16] Finally, as expected, steric hindrance appeared to play a minimal role with the samples treated at 900 °C, i.e., the DMZ and DEZ probes yielded essentially identical results at this temperature.

Table 3

LEIS peak areas from 3 keV He measurements of Si, O, and Zn on fused silica samples heated to the temperatures indicated in the table and then treated with one ALD cycle of DMZ or DEZ and water, fractional surface coverages ( $\vartheta$ ) of SiO<sub>2</sub> and ZnO, and the number of Si and Zn (SiOH) atoms/nm<sup>2</sup> on these surfaces. Prior to LEIS analysis, all samples were treated with 30 min of AO followed by annealing at 270 °C. The zinc and silicon signals from the ZnO and silica standards were 1627 and 586, respectively.

Sample	Si Raw Area	O Raw Area	Zn Raw Area	$\vartheta$ SiO <sub>2</sub>	$\vartheta$ ZnO	$\vartheta$ SiO <sub>2</sub> norm	$\vartheta$ ZnO norm	Si/nm <sup>2</sup>	Zn/nm <sup>2</sup> (SiOH/nm <sup>2</sup> )
DMZ 200 °C	460	520	794 ± 70	0.78	0.49	0.62	0.38	4.85	4.59 ± 0.25
DMZ 500 °C	566	557	376 ± 28	0.97	0.23	0.81	0.19	6.35	2.30 ± 0.14
DMZ 700 °C	531	550	230 ± 18	0.91	0.14	0.87	0.13	6.80	1.61 ± 0.11
DMZ 900 °C	595	527	87 ± 5	1.02	0.05	0.95	0.05	7.47	0.60 ± 0.03
DEZ 200 °C	486	525	756 ± 49	0.83	0.46	0.64	0.36	5.04	4.30 ± 0.18
DEZ 500 °C	569	541	306 ± 24	0.97	0.21	0.82	0.18	6.48	2.10 ± 0.21
DEZ 700 °C	582	546	169 ± 16	0.99	0.10	0.91	0.09	7.12	1.13 ± 0.09
DEZ 900 °C	597	550	91 ± 6	1.02	0.06	0.95	0.05	7.45	0.63 ± 0.04

### 3.7. What at the fused silica surface is reacting with DMZ and DEZ?

ALD reagents like DMZ are extremely reactive – it has been observed that such reagents should be capable of reacting with both surface silanols (SiOH moieties) and siloxanes (Si-O-Si groups). [50] Indeed, there appears to be a thermodynamic (enthalpic) driving force for both of these reactions because of the weak Zn-C bonds in DMZ and the stronger bonds that are expected to form from its reaction with either SiOH or Si-O-Si groups. However, a thermodynamic driving force for a reaction does always imply good kinetics. Hydroxylated fused silica surfaces that had been thermally treated at 200 °C were exposed to a single cycle of DMZ for either 30 ms or 50 ms. The resulting Zn 2p/Si 2p XPS narrow scan ratios for these surfaces were 0.2115 and 0.2186, respectively. These essentially identical results are consistent with a selective tagging of the surface silanols. That is, if DMZ were reacting with surface siloxanes, a longer exposure of a silica surface to this reagent should increase the Zn surface concentration, especially since, as shown in Table 3, DMZ tags less than half the surface (62 % of the tagged 200 °C surface is SiO<sub>2</sub>). Because of both these reasons and the results presented above, we conclude that, for kinetic reasons, DMZ and DEZ (i) are selective tagging agents for surface silanols on fused silica under the conditions described in this work and (ii) are not decomposing on our surfaces.

## 4. Conclusions

We have presented a tag-and-count approach for determining the densities of surface silanols on planar fused silica that couples ALD and HS-LEIS, where DMZ and DEZ were used to tag surface silanols with zinc by ALD, and HS-LEIS offered true surface sensitivity. Because of its relatively high mass, zinc, as a tagging agent, provides effective discrimination in LEIS between tagged surface silanols and the remaining atoms at the topmost layer of the material. DMZ, which is smaller and less sterically hindered than DEZ, gives somewhat more accurate results. However, all of the results in this study (both from the different thermal treatments and different tagging agents) are consistent with literature precedent. Using this methodology with DMZ, we obtained a value of 4.59 OH/nm<sup>2</sup> for fully hydroxylated fused silica. These results suggest that this approach may be able to determine surface hydroxyl densities on other glasses. Indeed, this methodology may be a useful tool for studying the surface chemistry of both glass surfaces and the early stages of ALD film growth.

### CRedit authorship contribution statement

**Tahereh G. Avval** : Conceptualization, Methodology, Investigation, Writing – original draft, Writing – review & editing. **Stanislav Průša** : Conceptualization, Investigation, Writing – original draft, Writing – review & editing, Supervision, Project administration. **Cody V. Cushman** : Conceptualization. **Grant T. Hodges** : Inves-

tigation. **Sarah Fearn** : Investigation. **Seong Kim** : Conceptualization. **Jan Čechal** : Investigation. **Elena Vaníčková** : Investigation. **Pavel Bábík** : Investigation. **Tomáš Šíkola** : Funding acquisition. **Hidde H. Brongersma** : Conceptualization, Methodology, Writing – original draft, Writing – review & editing, Supervision, Project administration. **Matthew R. Linford** : Conceptualization, Methodology, Writing – original draft, Writing – review & editing, Supervision, Project administration, Funding acquisition.

### Declaration of Competing Interest

The authors declare that they have no known competing financial interests or personal relationships that could have appeared to influence the work reported in this paper.

### Data availability

Data will be made available on request.

### Acknowledgment

CzechNanoLab project LM2018110 funded by MEYS CR is gratefully acknowledged for the financial support of the measurements at CEITEC Nano Research Infrastructure. We would also like to acknowledge the contributions of the following BYU undergraduate students: Jeffrey Chapman, Sean Chapman, and Victoria Carver.

### References

- [1] S.-W. Hung, J.-M. Tsai, M.-J. Cheng, P.-C. Chen, Analysis of the development strategy of late-entrants in Taiwan and Korea's TFT-LCD industry, *Technol. Soc.* 34 (1) (2012) 9–22, <https://doi.org/10.1016/j.techsoc.2011.12.001>.
- [2] Y.S. Choi, J.U. Yum, S.E. Park, Flat panel display glass: current status and future, *J. Non-Cryst. Solids* 431 (2016) 2–7, <https://doi.org/10.1016/j.jnoncrystol.2015.05.007>.
- [3] M.L. Hair, Hydroxyl groups on silica surface, *J. Non-Cryst. Solids* 19 (1975) 299–309, [https://doi.org/10.1016/0022-3093\(75\)90095-2](https://doi.org/10.1016/0022-3093(75)90095-2).
- [4] S. Takeda, K. Yamamoto, Y. Hayasaka, K. Matsumoto, Surface OH group governing wettability of commercial glasses, *J. Non-Cryst. Solids* 249 (1) (1999) 41–46, [https://doi.org/10.1016/S0022-3093\(99\)00297-5](https://doi.org/10.1016/S0022-3093(99)00297-5).
- [5] G. Agnello, J. Hamilton, R. Manley, E. Streltsova, W. LaCourse, A. Cormack, Investigation of contact-induced charging kinetics on variably modified glass surfaces, *Appl. Surf. Sci.* 356 (2015) 1189–1199, <https://doi.org/10.1016/j.apsusc.2015.08.208>.
- [6] J.J. Stapleton, D.L. Suchy, J. Banerjee, K.T. Mueller, C.G. Pantano, Adsorption reactions of carboxylic acid functional groups on sodium aluminosilicate glass fiber surfaces, *ACS Appl. Mater. Interfaces* 2 (11) (2010) 3303–3309, <https://doi.org/10.1021/am100730z>.
- [7] D.E. Mentley, State of flat-panel display technology and future trends, *Proc. IEEE* 90 (4) (2002) 453–459, <https://doi.org/10.1109/JPROC.2002.1002520>.
- [8] C.V. Cushman, J. Zakel, B.S. Sturgell, G.I. Major, B.M. Lunt, P. Brüner, T. Grehl, N.J. Smith, M.R. Linford, Time-of-flight secondary ion mass spectrometry of wet and dry chemically treated display glass surfaces, *J. Am. Ceram. Soc.* 100 (10) (2017) 4770–4784.
- [9] C.V. Cushman, P. Brüner, J. Zakel, C. Dahlquist, B. Sturgell, T. Grehl, B.M. Lunt, J. Banerjee, N.J. Smith, M.R. Linford, Low energy ion scattering (LEIS) of as-formed and chemically modified display glass and peak-fitting of the Al/Si LEIS peak envelope, *Appl. Surf. Sci.* 455 (2018) 18–31, <https://doi.org/10.1016/j.apsusc.2018.04.127>.
- [10] A.S. D'Souza, C.G. Pantano, K.M.R. Kallury, Determination of the surface silanol concentration of amorphous silica surfaces using static secondary ion mass spectrometry, *J. Vac. Sci. Technol., A* 15 (3) (1997) 526–531, <https://doi.org/10.1116/1.580678> (accessed 2021/08/07).
- [11] A.M. Schrader, J.L. Monroe, R. Sheil, H.A. Dobbs, T.J. Keller, Y. Li, S. Jain, M.S. Shell, J.N. Israelachvili, S. Han, Surface chemical heterogeneity modulates silica surface hydration, *Proc. Natl. Acad. Sci. U.S.A.* 115 (12) (2018) 2890–2895.
- [12] L.T. Zhuravlev, The surface chemistry of amorphous silica. Zhuravlev model, *Colloids Surf., A* 173 (1) (2000) 1–38, [https://doi.org/10.1016/S0927-7757\(00\)00556-2](https://doi.org/10.1016/S0927-7757(00)00556-2).
- [13] H. Pulker, H. Pulker, *Coatings on Glass*, Elsevier, 1999.
- [14] J. Erkelens, B.G. Linsen, Quantitative determination of hydroxyl groups and water for silica, *Journal of Colloid and Interface Science* 29 (3) (1969) 464–468, doi: 10.1016/0021-9797(69)90128-3; J.-P. Gallas, J.-M. Goupil, A. Vimont, J.-C. Lavalley, B. Gil, J.-P. Gilson, O. Miserque, Quantification of water and silanol species on various silicas by coupling IR spectroscopy and in-situ thermogravimetry, *Langmuir* 25 (2009) (10) 5825–5834, doi: 10.1021/la802688w; C.G. Armistead, A.J. Tyler, F.H. Hambleton, S.A. Mitchell, J.A. Hockey, Surface hydroxylation of silica, *J. Phys. Chem.* 73 (11) (1969) 3947–3953, doi: 10.1021/j100845a065.
- [15] R.S. McDonald, Surface functionality of amorphous silica by infrared spectroscopy, *J. Phys. Chem.* 62 (10) (1958) 1168–1178, doi: 10.1021/j150568a004; J.H. Anderson, K.A. Wickersheim, Near infrared characterization of water and hydroxyl groups on silica surfaces, *Surface Sci.* 2 (1964) 252–260, doi: 10.1016/0039-6028(64)90064-0.
- [16] L. Zhuravlev, The surface chemistry of amorphous silica. Zhuravlev model, *Colloids Surf. A* 173 (1–3) (2000) 1–38.
- [17] M.L. Hair, Hydroxyl groups on silica surface, in: D.E. Day (Ed.), *Glass Surfaces*, Elsevier, 1975, pp 299–309.
- [18] V.V. Potapov, L.T. Zhuravlev, Concentration of various forms of water in silica precipitated from a hydrothermal solution, *J. Volcanol. Seismolog.* 1 (5) (2007) 310–318, <https://doi.org/10.1134/S074204630705003X>.
- [19] L.T. Zhuravlev, V.V. Potapov, Density of silanol groups on the surface of silica precipitated from a hydrothermal solution, *Russ. J. Phys. Chem.* 80 (7) (2006) 1119–1128, <https://doi.org/10.1134/S0036024406070211>.
- [20] J. Banerjee, V. Bojan, C.G. Pantano, S.H. Kim, Effect of heat treatment on the surface chemical structure of glass: oxygen speciation from in situ XPS analysis, *J. Am. Ceram. Soc.* 101 (2) (2018) 644–656 <https://doi.org/10.1111/jace.15245> (accessed 2021/08/11).
- [21] C.V. Cushman, *Multi-Instrument Surface Characterization of Display Glass*, Brigham Young University, 2019.
- [22] H. Bach, Advanced surface analysis of silicate glasses, oxides and other insulating materials: a review, *J. Non-Cryst. Solids* 209 (1–2) (1997) 1–18.
- [23] Cushman, C. V. Multi-Instrument Surface Characterization of Display Glass, 2019.
- [24] V. Dugas, Y. Chevalier, Surface hydroxylation and silane grafting on fumed and thermal silica, *J. Colloid Interface Sci.* 264 (2) (2003) 354–361, [https://doi.org/10.1016/S0021-9797\(03\)00552-6](https://doi.org/10.1016/S0021-9797(03)00552-6).
- [25] A. Myalitsin, S.-h. Urashima, S. Nihonyanagi, S. Yamaguchi, T. Tahara, Water structure at the buried silica/aqueous interface studied by heterodyne-detected vibrational sum-frequency generation, *J. Phys. Chem. C* 120 (17) (2016) 9357–9363, doi: 10.1021/acs.jpcc.6b03275; O. Isaienko, E. Borguet, Hydrophobicity of hydroxylated amorphous fused silica surfaces, *Langmuir* 29 (25) (2013) 7885–7895, doi: 10.1021/la401259r; H.-F. Fan, F. Li, R.N. Zare, K.-C. Lin, Characterization of two types of silanol groups on fused-silica surfaces using evanescent-wave cavity ring-down spectroscopy, *Anal. Chem.* 79 (10) (2007) 3654–3661, doi: 10.1021/ac062386n.
- [26] D. Sprenger, H. Bach, W. Meisel, P. Gütlisch, XPS study of leached glass surfaces, *J. Non-Crystalline Solids* 126 (1) (1990) 111–129, doi: 10.1016/0022-3093(90)91029-Q; Y. Hayashi, K. Matsumoto, Determination of surface silanol group on silicate glasses using static SIMS, *J. Ceram. Soc. Jpn* 100 (1164) (1992) 1038–1041.
- [27] L.A. Langley, D.E. Villanueva, D.H. Fairbrother, Quantification of surface oxides on carbonaceous materials, *Chem. Mater.* 18 (1) (2006) 169–178, <https://doi.org/10.1021/cm051462k>.
- [28] C.V. Cushman, P. Brüner, J. Zakel, G.H. Major, B.M. Lunt, N.J. Smith, T. Grehl, M.R. Linford, Low energy ion scattering (LEIS). A practical introduction to its theory, instrumentation, and applications, *Anal. Methods* 8 (17) (2016) 3419–3439, <https://doi.org/10.1039/C6AY00765A>, 10.1039/C6AY00765A.
- [29] H.H. Brongersma, M. Draxler, M. de Ridder, P. Bauer, Surface composition analysis by low-energy ion scattering, *Surf. Sci. Rep.* 62 (3) (2007) 63–109, <https://doi.org/10.1016/j.surfrep.2006.12.002>.
- [30] A. Celaya Sanfiz, T.W. Hansen, A. Sakthivel, A. Trunskche, R. Schlögl, A. Knoester, H.H. Brongersma, M.H. Looi, S.B.A. Hamid, How important is the (001) plane of M1 for selective oxidation of propane to acrylic acid? *J. Catal.* 258 (1) (2008) 35–43, <https://doi.org/10.1016/j.jcat.2008.05.028>.
- [31] H.R.J. ter Veen, T. Kim, I.E. Wachs, H.H. Brongersma, Applications of high sensitivity low energy ion scattering (HS-LEIS) in heterogeneous catalysis, *Catal. Today* 140 (3) (2009) 197–201, doi: 10.1016/j.cattod.2008.10.012; H.H. Brongersma, T. Grehl, P.A. van Hal, N.C.W. Kuijpers, S.G.J. Mathijssen, E.R. Schofield, R.A.P. Smith, H.R.J. ter Veen, High-sensitivity and high-resolution low-energy ion scattering, *Vacuum* 84 (8) (2010) 1005–1007, doi: 10.1016/j.vacuum.2009.11.016; H. Téllez, A. Aguadero, J. Druce, M. Burriel, S. Fearn, T. Ishihara, D.S. McPhail, J.A. Kilner, New perspectives in the surface analysis of energy materials by combined time-of-flight secondary ion mass spectrometry (ToF-SIMS) and high sensitivity low-energy ion scattering (HS-LEIS), *J. Anal. Atomic Spectrometry* 29 (8) (2014) 1361–1370, doi: 10.1039/C3JA50292A; S. Průša, P. Procházka, P. Bábó, T. Šíkola, R. ter Veen, M. Fartmann, T. Grehl, P. Brüner, D. Roth, P. Bauer, et al., Highly sensitive detection of surface and intercalated impurities in graphene by LEIS, *Langmuir* 31 (35) (2015) 9628–9635, doi: 10.1021/acs.langmuir.5b01935.
- [32] J.M. McCrate, J.G. Ekerdt, Titration of free hydroxyl and strained siloxane sites on silicon dioxide with fluorescent probes, *Langmuir* 29 (38) (2013) 11868–11875, doi: 10.1021/la402825t; P. Chevallier, M. Castonguay, S. Turgeon, N. Dubrulle, D. Mantovani, P.H. McBreen, J.C. Wittmann, G. Laroche, Ammonia RF-plasma on PTFE surfaces: chemical characterization of the species created on the surface by vapor-phase chemical derivatization, *J. Phys. Chem. B* 105 (50) (2001) 12490–12497, doi: 10.1021/jp011607k.
- [33] Y. Xing, N. Dementev, E. Borguet, Chemical labeling for quantitative characterization of surface chemistry, *Curr. Opin. Solid State Mater. Science* 11 (5) (2007) 86–91, doi: 10.1016/j.cossms.2008.07.002; P. Van Der Voort, S. Vercauteren, K. Peeters, E.F. Vansant, Some precautions when determining the silanol number, using chemical modification with methylchlorosilanes, *J. Colloid Interface Sci.* 157 (2) (1993) 518–519, doi: 10.1006/jcis.1993.1219; Chapter 8 Chemical modification of silica: applications and procedures, in: E.F. Vansant, P.



- Van Der Voort, K.C. Vrancken (Eds.), *Studies in Surface Science and Catalysis*, Vol. 93, Elsevier, 1995, pp 149–192; V. Povstugar, S. Mikhailova, A. Shakov, Chemical derivatization techniques in the determination of functional groups by X-ray photoelectron spectroscopy, *J. Anal. Chem.* 55 (5) (2000) 405–416.
- [34] R.L. Puurunen, Surface chemistry of atomic layer deposition: a case study for the trimethylaluminum/water process, *J. Appl. Phys.* 97 (12) (2005) 121301, <https://doi.org/10.1063/1.1940727> (accessed 2021/08/13).
- [35] D. Shah, D.I. Patel, T. Roychowdhury, G.B. Rayner, N. O'Toole, D.R. Baer, M.R. Linford, Tutorial on interpreting x-ray photoelectron spectroscopy survey spectra: Questions and answers on spectra from the atomic layer deposition of Al<sub>2</sub>O<sub>3</sub> on silicon, *J. Vacuum Sci. Technol. B* 36 (6) (2018) 062902, doi: 10.1116/1.5043297 (accessed 2021/08/13); D. Shah; D.I. Patel, T. Roychowdhury, D. Jacobsen, J. Erickson, M.R. Linford, Optical function of atomic layer deposited alumina (0.5–41.0 nm) from 191 to 1688 nm by spectroscopic ellipsometry with brief literature review, *Surface Sci. Spectra* 26 (2) (2019) 026001, doi: 10.1116/1.5114827 (accessed 2021/08/13); M.D. Groner, F.H. Fabreguette, J.W. Elam, S.M. George, Low-temperature Al<sub>2</sub>O<sub>3</sub> atomic layer deposition, *Chem. Mater.* 16 (4) (2004) 639–645, doi: 10.1021/cm0304546; E. Ghiraldelli, C. Pelosi, E. Gombia, G. Chiavarotti, L. Vanzetti, ALD growth, thermal treatments and characterisation of Al<sub>2</sub>O<sub>3</sub> layers, *Thin Solid Films* 517 (1) (2008) 434–436, doi: 10.1016/j.tsf.2008.08.052.
- [36] E. Guziewicz, M. Godlewski, T. Krajewski, L. Wachnicki, A. Szczepanik, K. Kopalko, A. Wójcik-Głodowska, E. Przeździecka, W. Paszkowicz, E. Łusakowska, P. Kruszewski, N. Huby, G. Tallarida, S. Ferrari, ZnO grown by atomic layer deposition: A material for transparent electronics and organic heterojunctions, *J. Appl. Phys.* 105 (12) (2009) 122413.
- [37] L. Wachnicki, M. Łukasiewicz, B. Witkowski, T. Krajewski, G. Luka, K. Kopalko, R. Minikayev, E. Przeździecka, J.Z. Domagała, M. Godlewski, E. Guziewicz, Comparison of dimethylzinc and diethylzinc as precursors for monocrystalline zinc oxide grown by atomic layer deposition method: Comparison of dimethylzinc and diethylzinc as precursors for monocrystalline ZnO, *Phys. Stat. Sol. (b)* 247 (7) (2010) 1699–1701.
- [38] G.P. Gakis, C. Vahlas, H. Vergnes, S. Dourdain, Y. Tison, H. Martinez, J. Bour, D. Ruch, A.G. Boudouvis, B. Caussat, et al., Investigation of the initial deposition steps and the interfacial layer of Atomic Layer Deposited (ALD) Al<sub>2</sub>O<sub>3</sub> on Si, *Appl. Surface Sci.* 492 (2019) 245–254, doi: 10.1016/j.apsusc.2019.06.215; A.M. Hoyas, C.M. Whelan, J. Schuhmacher, J.P. Celis, K. Maex, Effect of surface reactive site density and reactivity on the growth of atomic layer deposited WN[sub x]C[sub y] films, *Electrochem. Solid-State Lett.* 9 (7) (2006) F64, doi: 10.1149/1.2203239.
- [39] R.A. Synowicki, Suppression of backside reflections from transparent substrates, accessed 2021/12/20. *Physica Status Solidi C*. 5 (5) (2008) 1085–1088, <https://doi.org/10.1002/pssc.200777873>.
- [40] F.A. Stevie, C.L. Donley, Introduction to x-ray photoelectron spectroscopy, *J. Vac. Sci. Technol.*, A 38 (6) (2020), 063204 <https://doi.org/10.1116/6.0000412> (accessed 2021/08/18).
- [41] N. Madaan, S.S. Kanyal, D.S. Jensen, M.A. Vail, A.E. Dadson, M.H. Engelhard, H. Samha, M.R. Linford, Al<sub>2</sub>O<sub>3</sub> e-beam evaporated onto silicon (100)/SiO<sub>2</sub>, by XPS, *Surf. Sci. Spectra* 20 (1) (2013) 43–48 <https://doi.org/10.1116/11.20121102> (accessed 2021/12/31).
- [42] N. Fairley, V. Fernandez, M. Richard-Plouet, C. Guillot-Deudon, J. Walton, E. Smith, D. Flahaut, M. Greiner, M. Biesinger, S. Tougaard, D. Morgan, J. Baltrusaitis, Systematic and collaborative approach to problem solving using X-ray photoelectron spectroscopy, *Appl. Surface Sci. Adv.* 5 (2021) 100112.
- [43] M.H. Engelhard, D.R. Baer, A. Herrera-Gomez, P.M.A. Sherwood, Introductory guide to backgrounds in XPS spectra and their impact on determining peak intensities, *J. Vac. Sci. Technol.*, A 38 (6) (2020), 063203 <https://doi.org/10.1116/6.0000359> (accessed 2021/12/31).
- [44] J. Hilfiker, H. Tompkins, *Spectroscopic Ellipsometry: Practical Application to Thin Film Characterization*, 2016.
- [45] J. Liu, J. Bao, M. Scharnberg, W.C. Kim, P.S. Ho, R. Laxman, Effects of surface chemistry on ALD Ta<sub>3</sub>N<sub>5</sub> barrier formation on low-k dielectrics, *J. Vacuum Sci. Technol. A* 23 (4) (2005) 1107–1113, doi: 10.1116/1.1872012 (accessed 2021/12/21); E. Langereis, J. Keijmel, M.C.M. van de Sanden, W.M.M. Kessels, Surface chemistry of plasma-assisted atomic layer deposition of Al<sub>2</sub>O<sub>3</sub> studied by infrared spectroscopy, *Appl. Phys. Lett.* 92 (23) (2008) 231904, doi: 10.1063/1.2940598 (accessed 2021/12/21); R. Krumpolec, D.C. Cameron, T. Homola, M. Černák, Surface chemistry and initial growth of Al<sub>2</sub>O<sub>3</sub> on plasma modified PTFE studied by ALD, *Surf. Interfaces* 6 (2017) 223–228, doi: 10.1016/j.surfin.2016.10.005.
- [46] B. Xia, J.J. Ganem, E. Briand, S. Steydli, H. Tancrez, I. Vickridge, The carbon and hydrogen contents in ALD-grown ZnO films define a narrow ALD temperature window, *Vacuum* 190 (2021) 110289, <https://doi.org/10.1016/j.vacuum.2021.110289>.
- [47] W. Chen, Y.H. Lu, M. Wang, L. Kroner, H. Paul, H.-J. Fecht, J. Bednarcik, K. Stahl, Z.L. Zhang, U. Wiedwald, U. Kaiser, P. Ziemann, T. Kikegawa, C.D. Wu, J.Z. Jiang, Synthesis, thermal stability and properties of ZnO<sub>2</sub> nanoparticles, *J. Phys. Chem. C* 113 (4) (2009) 1320–1324.
- [48] J.F. Moulder, *Handbook of X-ray photoelectron spectroscopy*, *Phys. Electron.* (1995) 230–232.
- [49] J. Cai, Z. Ma, U. Wejinya, M. Zou, Y. Liu, H. Zhou, X. Meng, A revisit to atomic layer deposition of zinc oxide using diethylzinc and water as precursors, *J. Mater. Sci.* 54 (7) (2019) 5236–5248, <https://doi.org/10.1007/s10853-018-03260-3>.
- [50] R.L. Puurunen, A. Root, S. Haukka, E.I. Iiskola, M. Lindblad, A.O.I. Krause, IR and NMR study of the chemisorption of ammonia on trimethylaluminum-modified silica, *J. Phys. Chem. B* 104 (28) (2000) 6599–6609, <https://doi.org/10.1021/jp000454i>.